

***Supporting Information***

Near-infrared Aggregation-Induced Emission Characteristics of New  
*o*-Carborane Fluorophores with Large Stokes Shifts and Self-  
recovering Mechanochromic Luminescence

Xueyan Wu, Na Li, Chenxi Zhang, Yan Lv, Jixi Guo\*

State Key Laboratory of Chemistry and Utilization of Carbon Based Energy  
Resources; College of Chemistry, Xinjiang University, Urumqi, 830017, Xinjiang, PR  
China

Email: [Wuxy90@xju.edu.cn](mailto:Wuxy90@xju.edu.cn), [jxguo1012@163.com](mailto:jxguo1012@163.com),

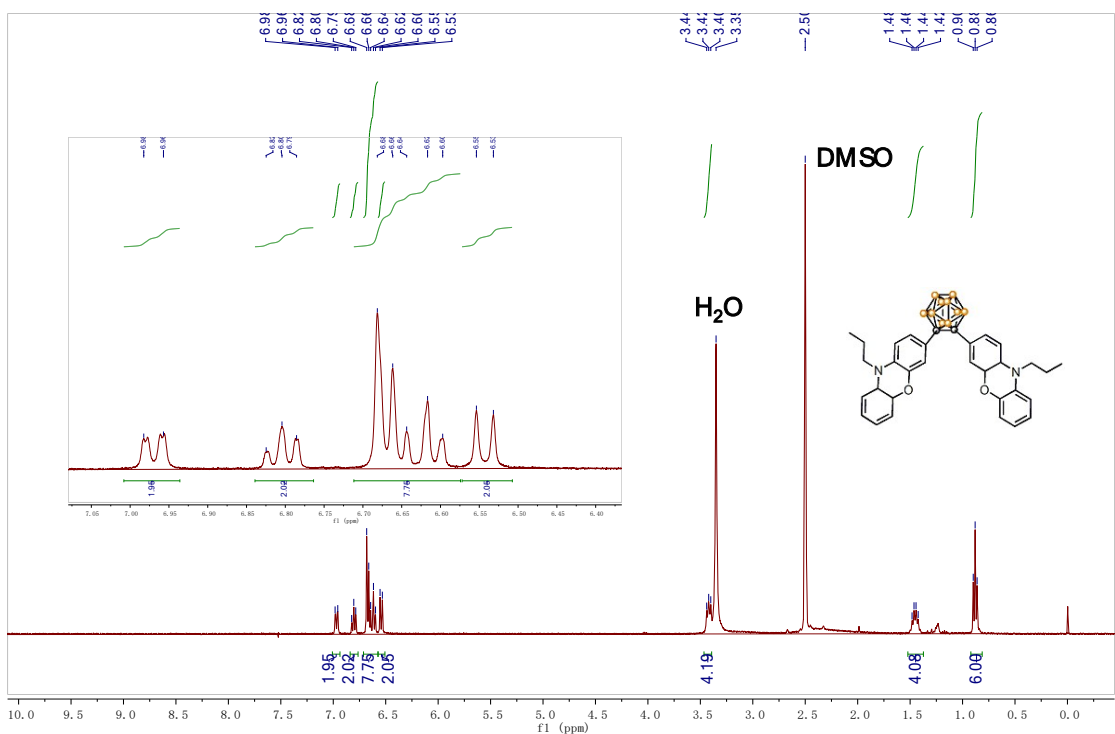


**Figure S1.** <sup>1</sup>H NMR spectra of CPO in  $\text{DMSO}-d_6$

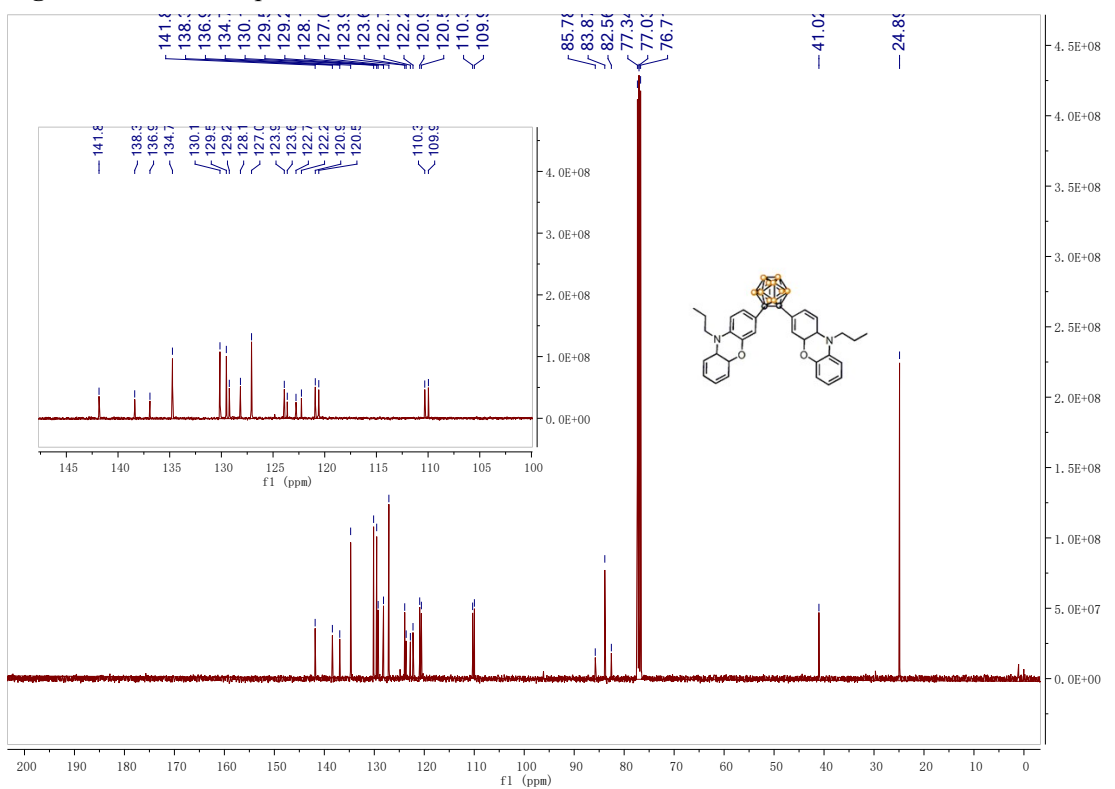


**Figure S2.** <sup>13</sup>C NMR spectra of CPO in  $\text{CDCl}_3$ .

CBPNO-ESH(500-700) #1 RT: 0.00 AV: 1 NL: 8.76E6  
T: FTMS - p ESI Full ms [500.0000-700.0000]

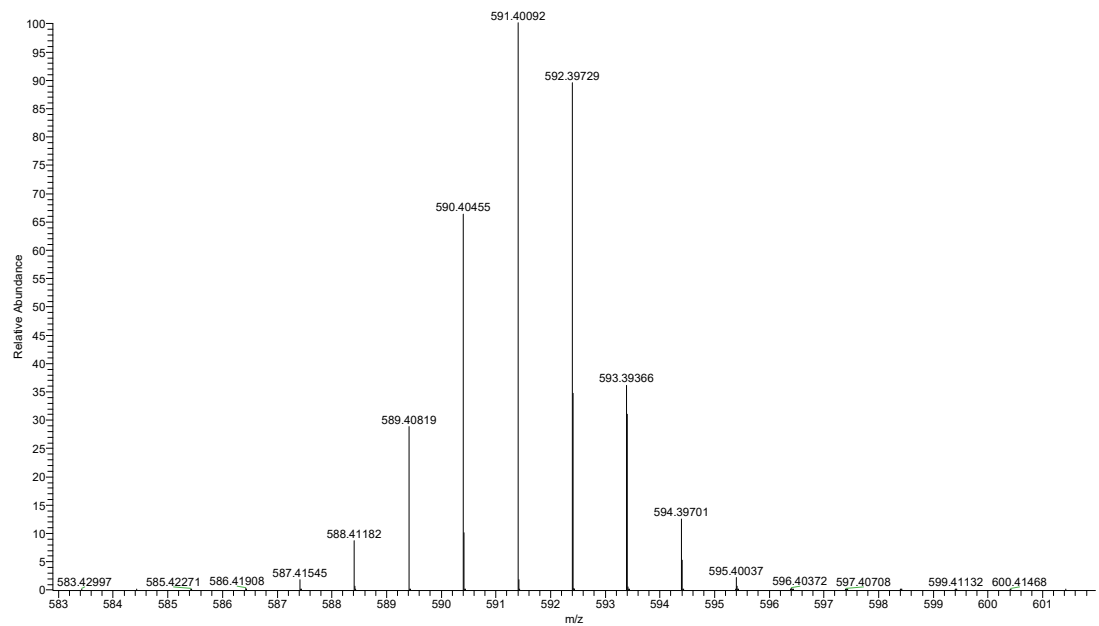


**Figure S3.** HRMS spectra of CPO

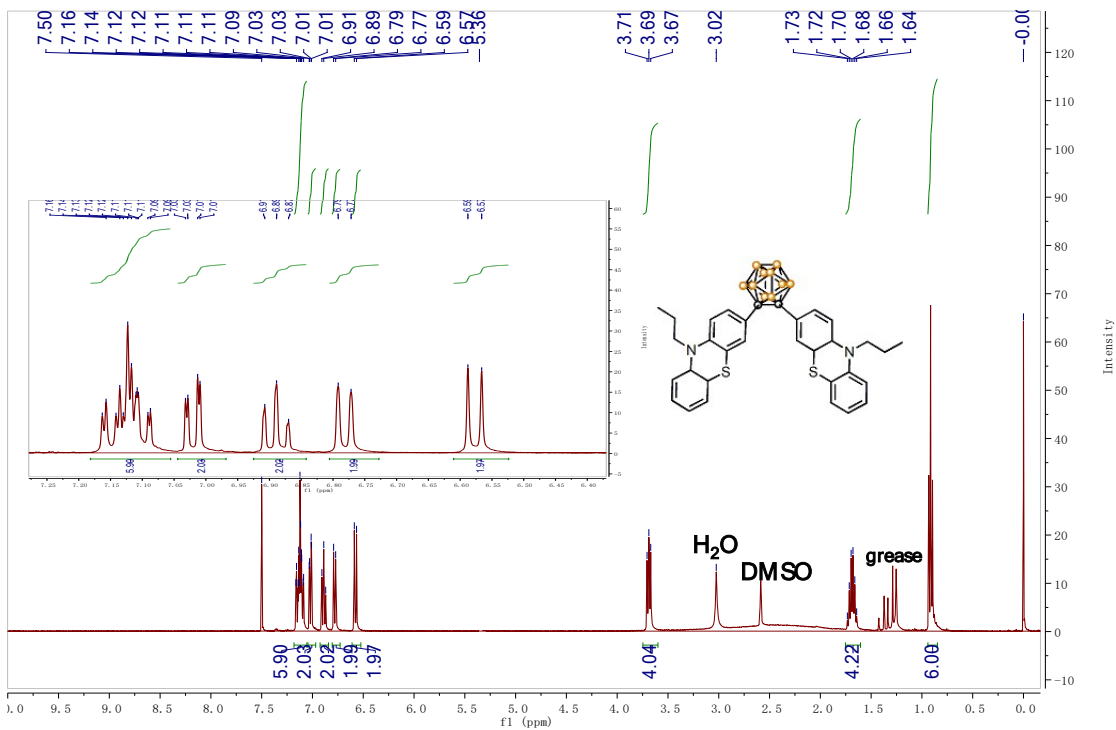


**Figure S4.** <sup>1</sup>H NMR spectra of CPS in CDCl<sub>3</sub> and DMSO-d<sub>6</sub>.

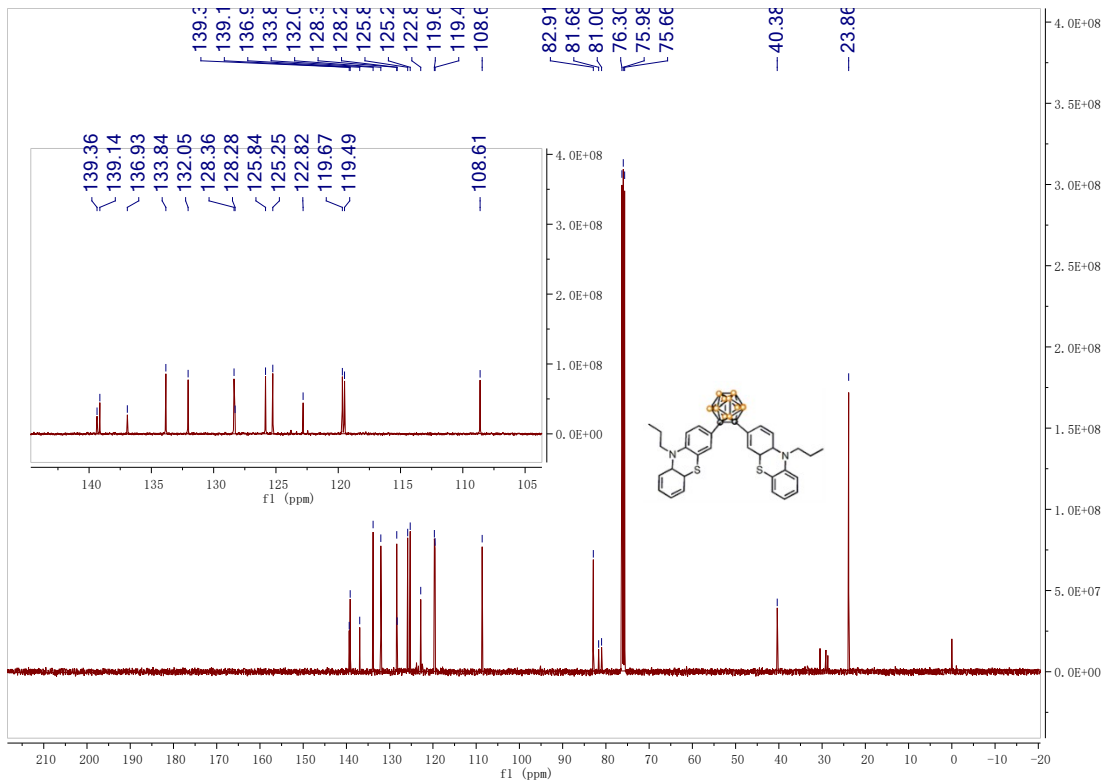


**Figure S5.**  $^{13}\text{C}$  NMR spectra of CPS in  $\text{CDCl}_3$ .

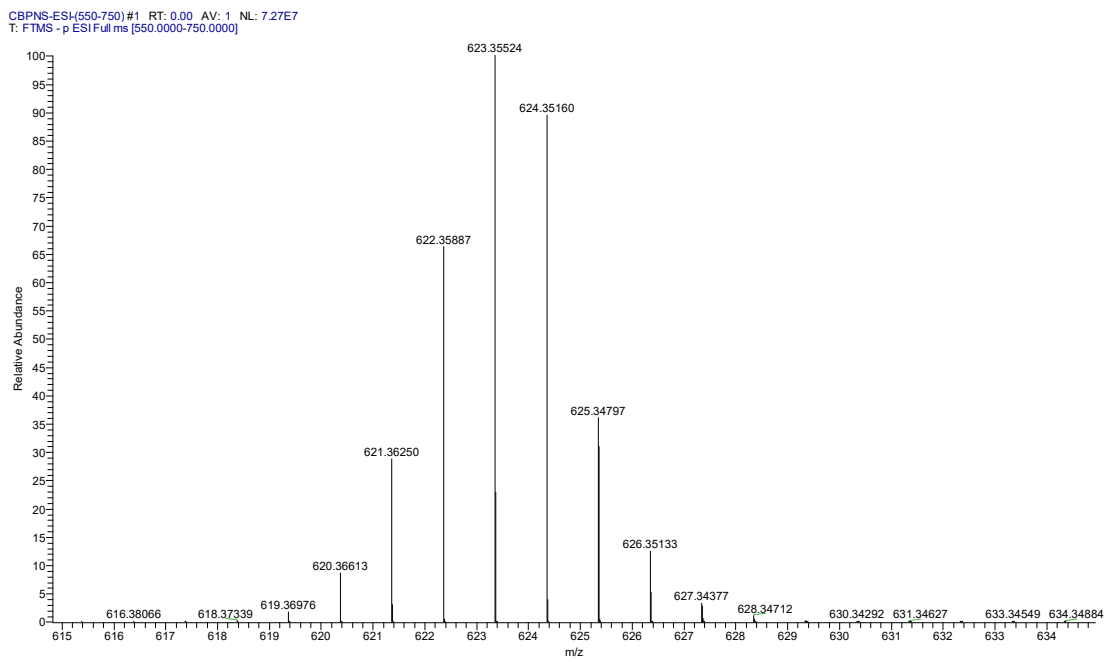


**Figure S6.** HRMS spectra of CPS

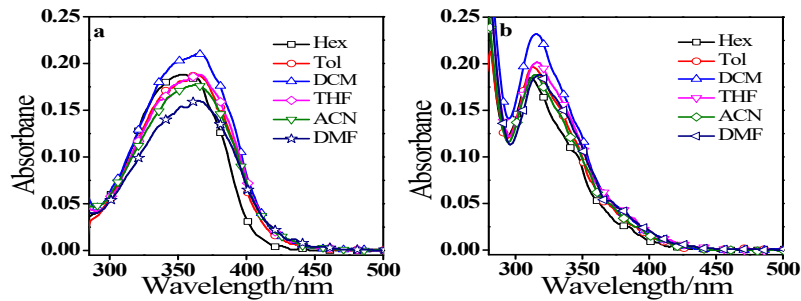


**Figure S7.** UV-Vis absorption spectra of (a) **CPO** and (b) **CPS** in different solvents.  $c = 1.0 \times 10^{-5}$  M, 20 °C.

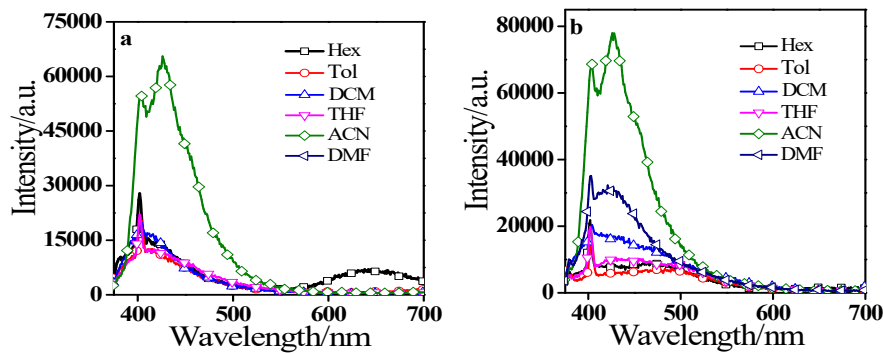


**Figure S8.** Fluorescence spectra of (a) **CPO** and (c) **CPS** in different solvents. ( $\lambda_{\text{ex}}=360\text{nm}$ ),  $c = 1.0 \times 10^{-5}$  M, 20 °C.

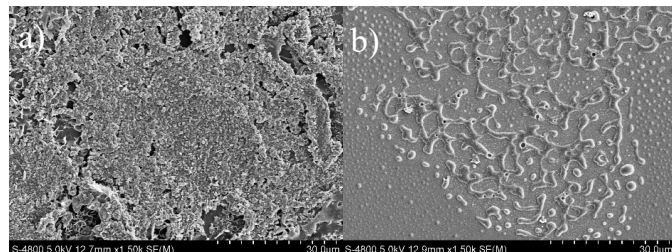


**Figure S9** SEM images of (a) **CPO** and (b) **CPS** with a 99% water fraction.

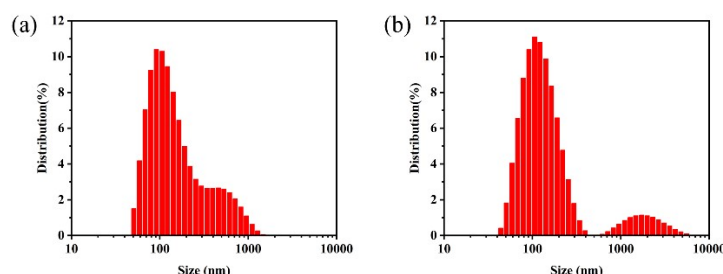


**Figure S10** Size distributions of nanoparticles of (a) **CPO** and (b) **CPS** with a 99% water fraction.

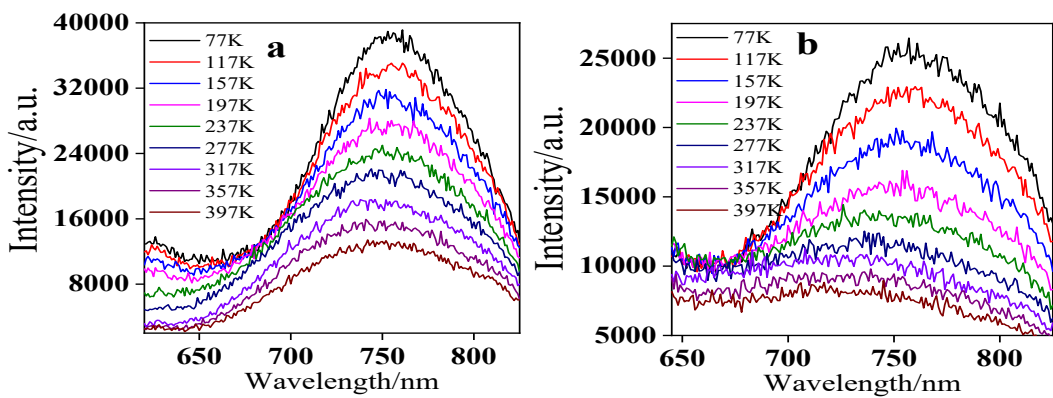


**Figure S11.** The normalized PL spectra of (a) **CPO** and (b) **CPS** in the solid state during heating from 77 to 397K.

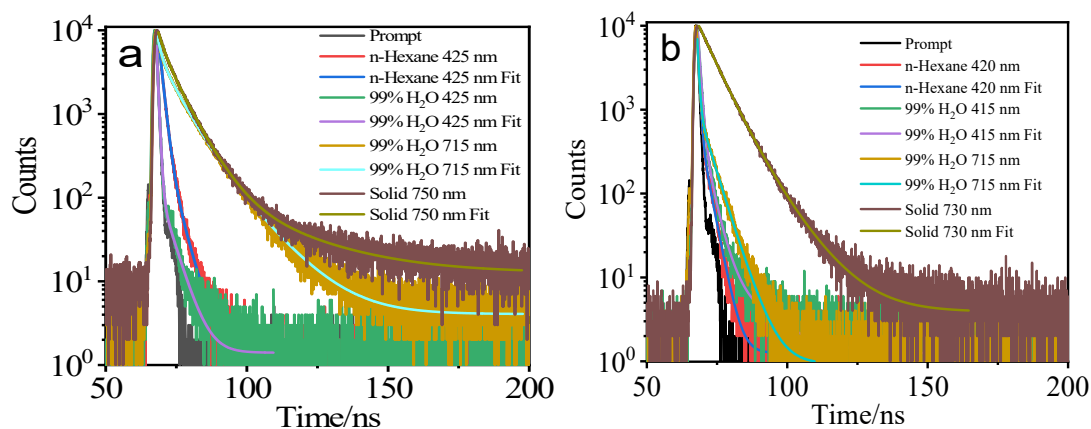


**Figure S12.** Decay profiles of fluorescence lifetime measurement of (a) **CPO** and (b) **CPS** in the solution, aggregation and solid state.

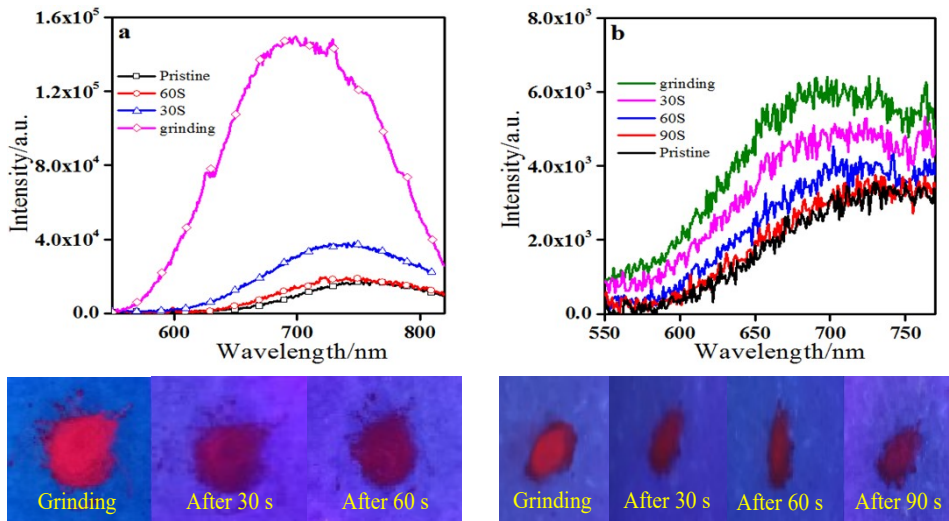


**Figure S13.** The self-recovering mechanochromic luminescence of (a) CPO and (b) CPS in solid at 60 °C, and the mechanochromic luminescence photographs of CPO and CPS changes with time under day and 365 nm UV light

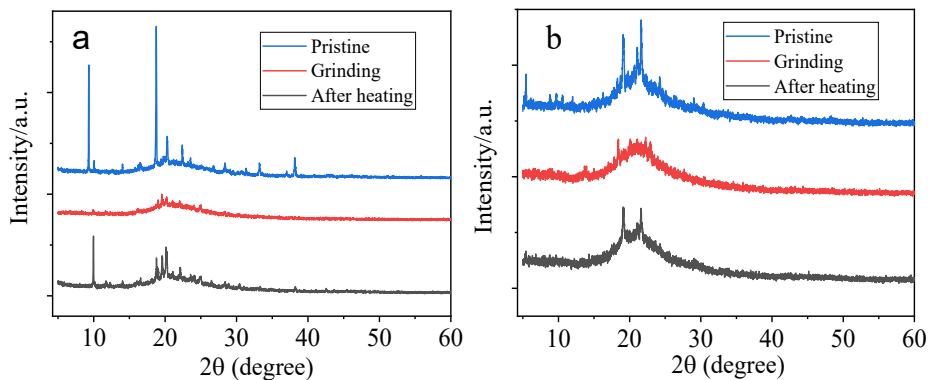


**Figure S14.** XRD patterns of CPO (a) CPS (b) in different solid-states: Pristine, Grinding and After heating.

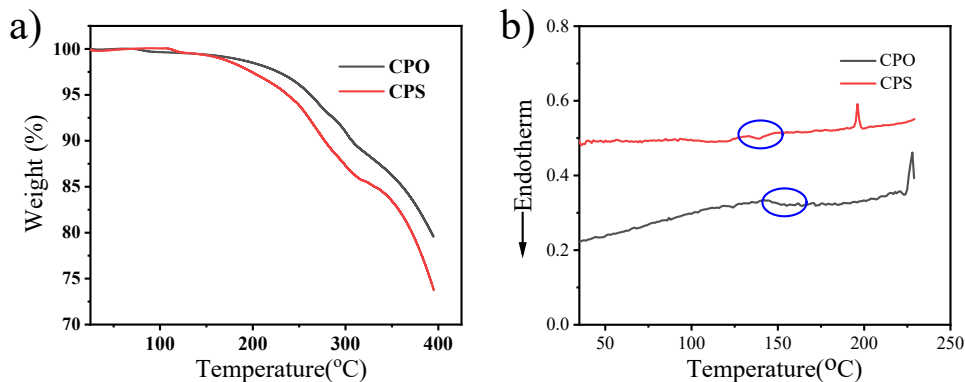


**Figure S15.** (a)TG and (b)DSC of CPO and CPS measured at a heating rate of 10 °C/min under N<sub>2</sub> atmosphere.

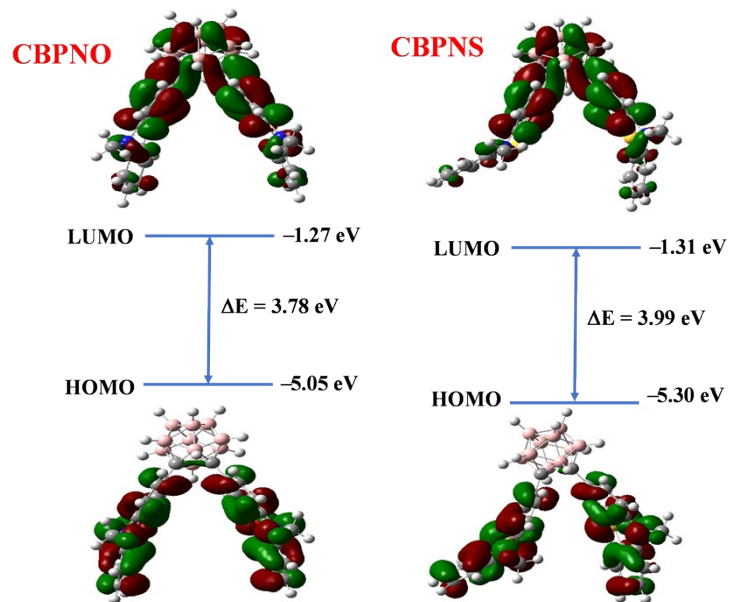


**Figure S16.** The electronic density contours and energy levels of the HOMOs and LUMOs of CPO and CPS were calculated by DFT at the B3LYP/6-31G(d,p) level with Gaussian 09W.

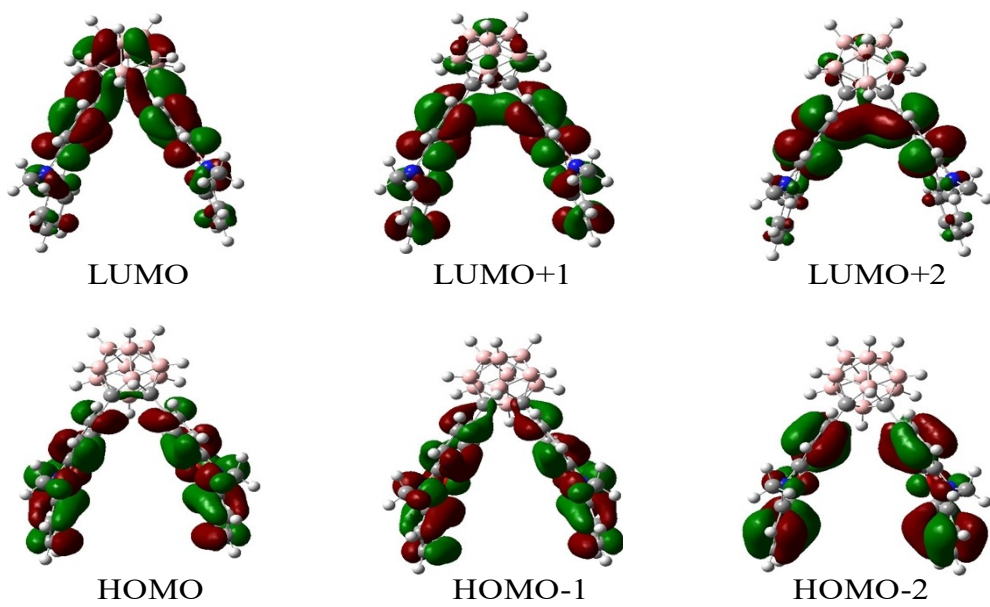


**Figure S17.** The theoretical calculated ground-state frontier orbitals contributions of CPO in gas state using B3LYP/6-31G (d, p) level by Gaussian 09.

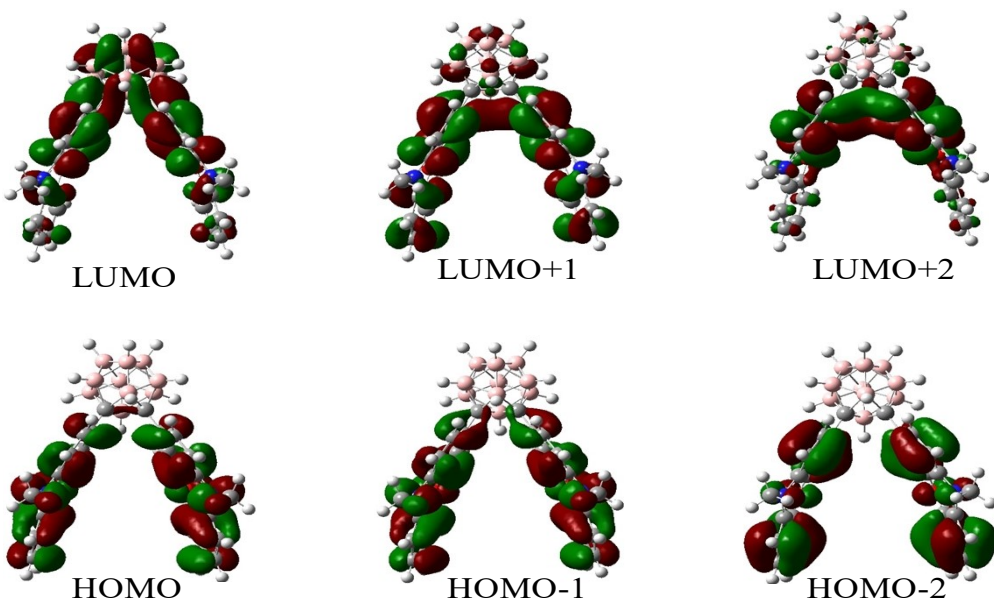


**Figure S18.** The theoretical calculated UV-vis absorption frontier orbitals contributions of **CPO** in gas state estimated by TD-DFT calculation at the B3LYP/6-31G (d, p) level by Gaussian 09.

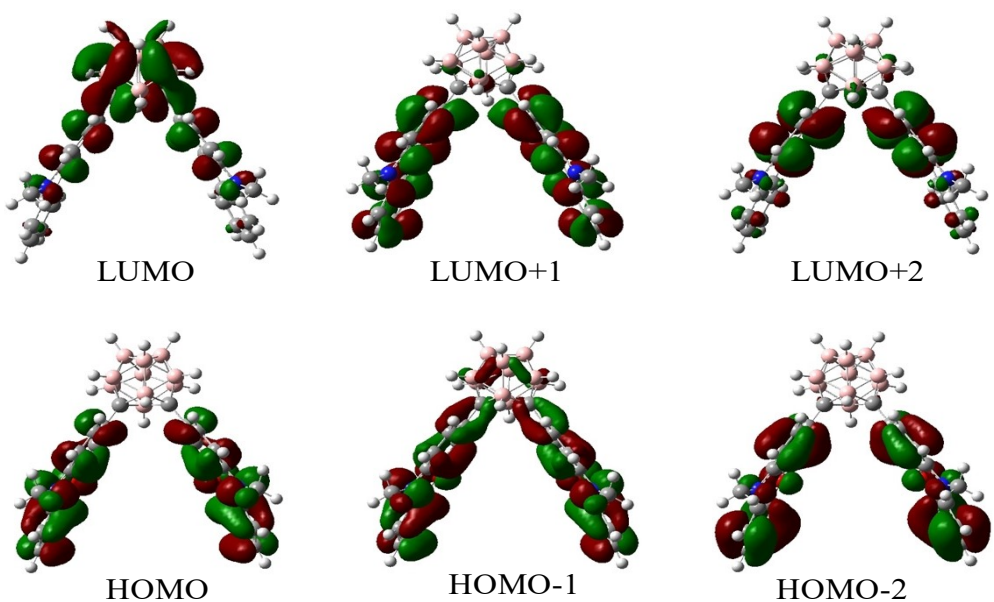


**Figure S19.** The theoretical calculated singlet state (Fluorescence) frontier orbitals contributions of **CPO** in gas state estimated by TD-DFT calculation at the B3LYP/6-31G (d, p) level by Gaussian 09.

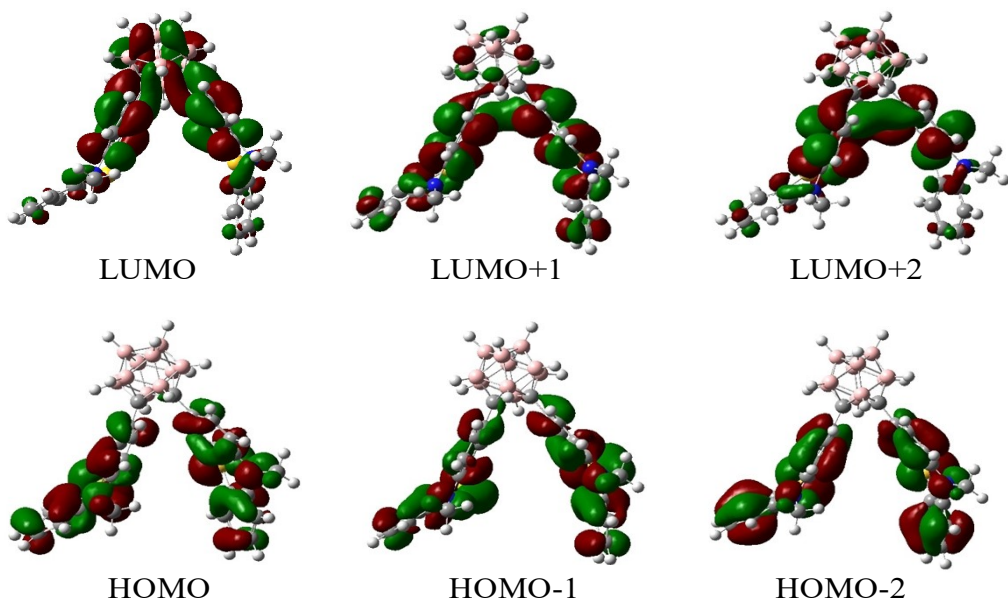


**Figure S20.** The theoretical calculated ground-state frontier orbitals contributions of **CPS** in gas state using B3LYP/6-31G (d, p) level by Gaussian 09.

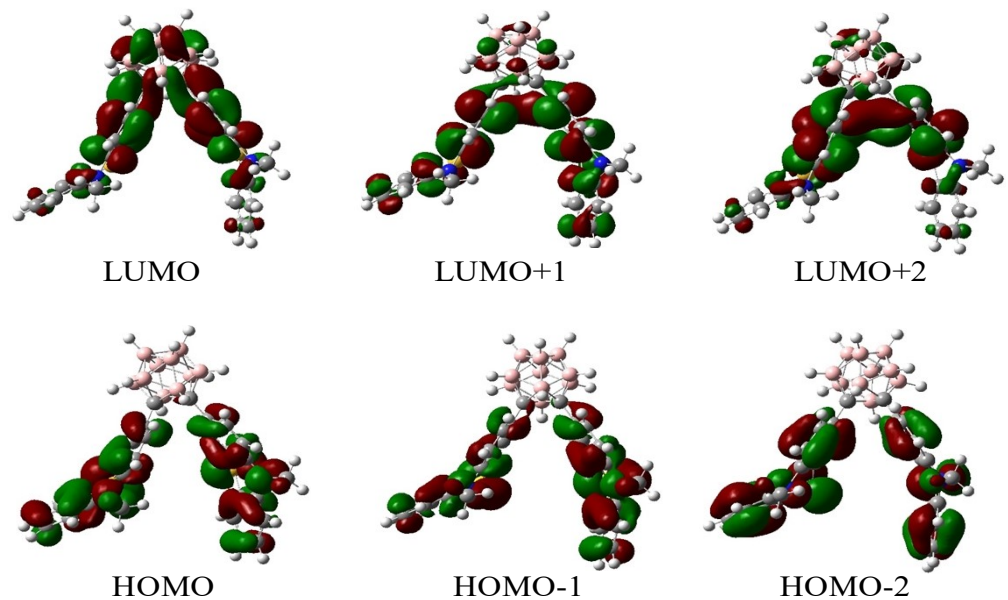


**Figure S21.** The theoretical calculated UV-Vis absorption frontier orbitals contributions of **CPS** in gas state estimated by TD-DFT calculation at the B3LYP/6-31G (d, p) level by Gaussian 09.

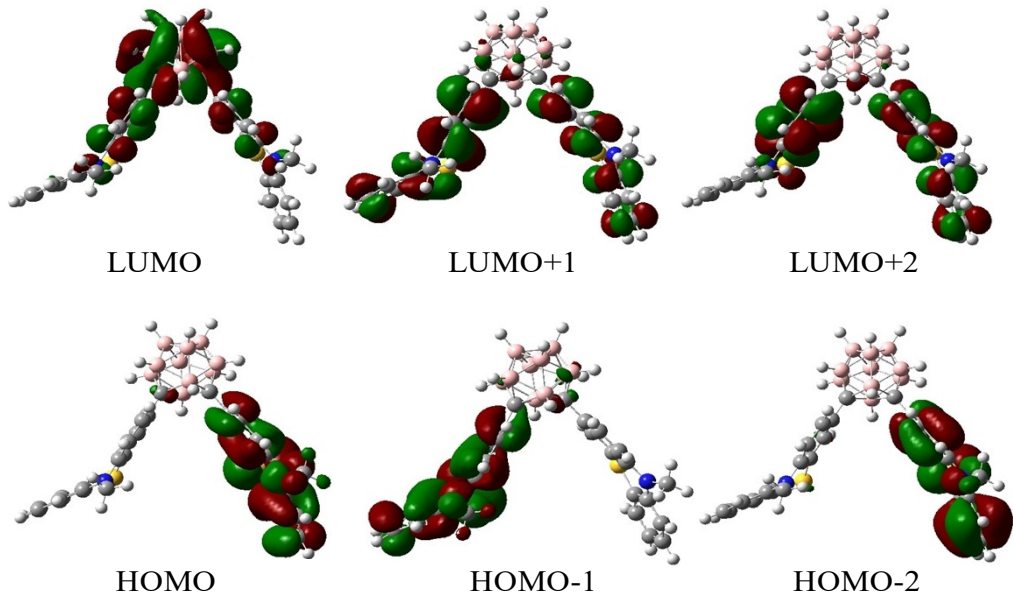


**Figure S22.** The theoretical calculated singlet state (Fluorescence) frontier orbitals contributions of **CPS** in gas state estimated by TD-DFT calculation at the B3LYP/6-31G (d, p) level by Gaussian 09.

**Table S1.** Selected parameters for the UV-vis absorption and Singlet state (Fluorescence) energy of the compounds. Electronic excitation energies (eV), oscillator strengths ( $f$ ), and configurations of the low-lying excited states of **CPO** and **CPS** were calculated using TD-DFT//B3LYP/6-31G(d, p), based on the optimized ground state geometries.

Compound	Transition type	Excitation energy <sup>a</sup>	$f$ <sup>b</sup>	Composition <sup>c</sup>	CI <sup>d</sup>
<b>CPO</b>	UV-Vis	$S_0 \rightarrow S_1$	3.2751 eV (379 nm)	H→L	0.6843
		$S_0 \rightarrow S_2$	3.3535 eV (370 nm)	H-1→L	0.6845
	Fluorescence	$S_0 \rightarrow S_1$	1.7305 eV (716 nm)	H→L	0.7063
<b>CPS</b>	UV-Vis	$S_0 \rightarrow S_1$	3.4373 eV (360 nm)	H→L	0.6557
		$S_0 \rightarrow S_2$	3.4856 eV (355 nm)	H-1→L	0.6464
	Fluorescence	$S_0 \rightarrow S_1$	1.4981 eV (827 nm)	H→L	0.7055

<sup>a</sup> Only selected excited states were considered. Numbers in parentheses are the excitation energy in wavelength. <sup>b</sup> Oscillator strength. <sup>c</sup> H stands for the HOMO and L stands for the LUMO. Only the main configurations are presented. <sup>d</sup> Coefficient of the wave function for each excitation. CI coefficients are given in absolute values.